OVERALL STUDY OF AIR/PROPANE COMBUSTION IN FLUIDIZED BEDS

Leonardo Ribeiro
Departamento de Eng. Mecânica. Instituto Superior de Engenharia do Porto. Rua Dr. António Bernardino de Almeida, 431
4200-072, Porto, Portugal
lsr@isep.ipp.pt

Carlos Pinho
CEFT-DEMEGI, Faculdade de Engenharia, Universidade do Porto, Rua Dr. Roberto Frias, s/n , 4200-465 Porto, Portugal
ctp@fe.up.pt

Abstract. Commercial propane was used to study the combustion of volatiles released from coal particles burning in fluidized beds. A set of experiments was made with four different sizes of sand particles. In these experiments mixtures of air and propane were blown into the fluidized bed through the distributor. The fluidized bed was heated with an electrical resistance placed around the reactor. The following measurements were made: the dry molar fractions of CO_2, CO and O_2 in the flue gases, the bed temperature and the intensity of the combustion noise. The objective was to determine the way fluidization disturbs the combustion mechanism of propane. For some experiments hematite, was introduced in the bed..A mathematical model concerning the tests performed without hematitet, was developed to evaluate the concentrations of chemical species and temperature in bubbles, clouds and particulate phase, and also the mass and energy transfer between bubbles and particulate phase. The comparison between numerical and experimental results allowed a better understanding of the combustion of volatiles inside fluidized beds.

Keywords. combustion, fluidized bed, propane, volatiles.

1. Introduction

When a batch of particles of coal is thrown into a hot fluidized bed, the particles release their volatile material and the remaining coke particles begin to burn. The volatiles released by coal particles consist mainly of H_2, CO, CH_4 and other higher hydrocarbons, Hesketh and Davidson (1991a and 1991b). The combustion of these higher hydrocarbons begins with their fragmentation into smaller hydrocarbons like propane, Westbrook and Dryer (1981), and because of this propane can represent well the volatiles released from coal. Consequently, the fuel used in this work was commercial propane with 91 % (w/w) of propane.

The explosions of propane and air mixtures in a fluidized bed can occur either inside the bed, at an unknown distance above the distributor, or above the free surface of the bed, Dennis et al. (1982), depending on the temperature. The temperature of the fluidized bed at which combustion takes place when the bubbles reach the free surface of the bed is known as critical temperature. For a bed hotter than the critical temperature, the bubbles burn inside the bed, while below the critical temperature the bubbles burn above the bed, (Dennis et al., 1982; Hayhurst, 1991; Ribeiro and Pinho, 1998; Hayhurst and Tucker, 1990).

Aoyagi and Kunii (1974) observed that the combustion of the volatiles released from coal particles burning inside fluidized beds takes place when these coal particles are inside the gas bubbles rising in the interior of the bed. In such situation and according to these authors, there is a flame around the burning coal particles and, as soon as the particles move into the clouds surrounding the bubbles, the flame extinguishes. Pillai (1981) studied the combustion of propane air mixtures in shallow beds and realized that the combustion reaction had to take place inside the bubble phase. Stubington et al. (1990) refer that the volatiles released from the coal particles either burn inside the bed or above its free surface. Hayhurst and Tucker (1990) and Hayhurst (1991) have shown that particles of coal burning in fluidized beds yield CO inside their own pores and that such CO burns in the bed, either inside the rising bubbles or above the free surface. Hayhurst (1991) has also shown that if the bed is composed by particles covered with platinum (catalyst), the CO formed at the surface of the coal particles by heterogeneous reactions burns in the particulate phase. Hesketh and Davidson (1991a) studied the combustion of coke in beds fluidized with mixtures of air and propane and concluded that the propane burns only inside the bubbles and never in the particulate phase. Hesketh and Davidson (1991b) studied also the combustion of stoichiometric mixtures of methane-air and propane-air in a bed working under incipient fluidizing conditions to find out if there were inhibition effects on the particulate phase for the gaseous phase combustion reactions.

Bulewicz et al. (1997), determined the composition of the off gases from shallow fluidized beds, with maximum depth of 15 mm, burning natural gas. They concluded that there is no connection between the composition of the flue gases and the sand size; that the CO concentration varied strongly with bed temperature at 900 ºC; and that the NO concentration varied with temperature, bed depth and excess air.

Hayhurst and Parmar (1998) have shown that the formed CO in a bed working in the temperature range of 1000 up to 1400 K, burns to CO_2 either inside the bubbles or above the bed. Above 1400 K the combustion of CO takes place near the particles from where it was formed. They have also shown that the combustion of CO takes place close to the particles of coal when the size of particles of sand is small.

Ribeiro and Pinho (1998) also studied the burning of stoichiometric mixtures of methane and propane with air and defined an incubation parameter to link the pre-ignition delay with an average bubble rising time. Such parameter can broadly be defined as a Damkholer number (Kanury, 1977; Williams, 1985; Borman and Ragland, 1998) for combustion inside the bubbles of a fluidized bed. Ribeiro and Pinho (2004) measured the concentrations of CO_2, CO and O_2 in the off gases and the noise level at the free board of deep fluidized beds, resulting from the combustion of pre-mixtures of propane and air. An overview of the curves of CO_2, CO and O_2 mole fractions, with the fluidized bed operating conditions, allowed the definition of four categories of operational conditions by taking into account common trends.

Hayhurst and Lawrence (1996) studied the combustion of C_5H_5N in fluidized beds. In their experiments the particulate phase was composed either by sand or a mixture of sand and CaO and the fluidizing gas used was a mixture of O_2 and N_2. The authors noticed that the presence of CaO in the particulate phase lowers the content of CO in the flue gases, but the kinetic mechanism that accelerates the burning of CO in the presence of CaO was not explained. Hayhurst and Lawrence (1997) studied, in a fluidized bed with particles of sand, the chemical reactions between iron and either iron oxides or the nitrogen oxides NO and N_2O. The fluidizing gas used was nitrogen; NO and N_2O were also blown into the fluidized bed.

Gokulakrishnan and Lawrence (1999) studied the combustion of C_5H_5N, mixed with traces of the catalyst HCl, in a fluidized bed of sand. The gas C_5H_5N was pre-mixed with HCl, and then this mixture was blown into the fluidized bed. The aim of the study was to determine the effect of HCl on the concentration of CO, NO_x and N_2O on the off gases. The authors concluded that HCl inhibits the creation of CO_2, but increases the yielding of CO. On the other hand, the authors also found that an increase of the temperature of the fluidized bed entails a lower yielding of CO.

2. Experimental installation

The fluidized bed was contained in a refractory steel tube of internal diameter of 80 mm with a stainless steel plate distributor with 101 holes (0.3 mm diameter), drilled according to a 7 mm square pitch, Ribeiro and Pinho (1998). For some experiments the fluidized material was silica sand of group B, Geldart (1986), with four different sizes: 400-500 µm, 315-400 µm, 250-315 µm and 200-250 µm. In the remaining experiments hematite, with a grain size of 420-500 µm, was mixed in the particulate phase with the sand 400-500 µm, in such a way to get 5% (w/w) of hematite in the particulate phase. The bed was heated up by a 4.2 kW electrical resistance, placed around the reactor tube and inserted in refractory clay pieces. Two K-thermocouples were used to measure the temperature at two different locations in the fluidized bed, and were connected to a data acquisition system. Another identical K-thermocouple was connected to the controller of temperature of the fluidized bed. The uncertainty associated with these thermocouples is the maximum of 2.2 ºC or 0.75 % of the reading. To measure the composition of the combustion gases, CO_2, CO and O_2 analyzers were used. The CO_2 and CO analyzers were of non-dispersive infrared type; their precision was 0.5 % of the maximum scale reading; the maximum of scale for the CO_2 analyzer was 25 % and for the CO analyzer was 5 %. The O_2 paramagnetic analyzer had a linearity better than 0.1 %; its precision was under 0.1 %; and the reading was affected at most 0.05 % by the battery charge. To measure the sound level yielded by the combustion it was used a sonometer from TES model 1351, with a range from 35 to 130 dB, precision of ±1.5 dB, resolution of 0.1 and a delay of 125 ms; the curve of ponderation used was suitable for sounds of low intensity.

The gas sampling and suction probe was made of stainless steel, 4 mm inner diameter and 5 m in length. The collected gases were cooled to 50 ºC before reaching the analyzers. The gas sampling and suction probe and the sonometer probe were placed about 10 cm above the bed at the fixed state. During each experiment the fluidized bed was heated from 400 to 900 ºC, and at every four seconds, the readings of the three analyzers of the flue gas, the sonometer and the arithmetic mean of the readings of the two thermocouples immersed in the bed, were recorded. More details on the experimental procedure can be seen at Ribeiro and Pinho (2004).

2. Experimental results

2.1. Combustion of pre-mixtures of propane and air

Experiments were performed with four different sizes (400-500, 315-400, 250-315 and 200-250 µm), five static bed heights (10, 15, 20, 25 and 30 cm) and three different mass flow rates of reactants, Tab. (1), with 0, 10, 20 and 30 % excess air, giving a total of 240 experiments.

The fluidized beds were hydrodynamically characterized, for a given temperature T, and each sand size used, through velocities $u(T)$, $u_{mf}(T)$, the *ratio* $u/u_{mf}(T)$ and also by the definition of the threshold temperature for the appearance of slugs. Table (1) gives, for all sand sizes, the mass flow-rates, the mole fractions of air and propane in all

mixtures injected into the fluidized bed, and equations for $u(T)$. Table (2) presents the ratio u/u_{mf} (T), for all experimentally studied situations.

Table 1. Mass flow-rates, mole fractions and $u(T)$. All sand sizes.

Excess Air	C_3H_8	Air	C_3H_8	Air	u/T
%	kg/min	kg/min	-	-	m/s/ K
0	1.073×10^{-3}	1.628×10^{-2}	0.040	0.960	1.596×10^{-4}
0	1.190×10^{-3}	1.778×10^{-2}	0.040	0.960	1.745×10^{-4}
0	1.305×10^{-3}	1.981×10^{-2}	0.040	0.960	1.943×10^{-4}
10	9.770×10^{-4}	1.628×10^{-2}	0.037	0.963	1.590×10^{-4}
10	1.073×10^{-3}	1.778×10^{-2}	0.037	0.963	1.738×10^{-4}
10	1.190×10^{-3}	1.981×10^{-2}	0.037	0.963	1.935×10^{-4}
20	9.040×10^{-4}	1.628×10^{-2}	0.034	0.966	1.586×10^{-4}
20	9.770×10^{-4}	1.778×10^{-2}	0.034	0.966	1.731×10^{-4}
20	1.097×10^{-3}	1.981×10^{-2}	0.034	0.966	1.930×10^{-4}
30	8.299×10^{-4}	1.628×10^{-2}	0.031	0.969	1.581×10^{-4}
30	9.040×10^{-4}	1.778×10^{-2}	0.031	0.969	1.727×10^{-4}
30	1.001×10^{-3}	1.981×10^{-2}	0.031	0.969	1.923×10^{-4}

Table 2. The *ratio $u/u_{mf}(T)$* for all situations experimentally studied.

Sand size	Air flow rate 1.628×10^{-2} (kg/min)	Air flow rate 1.778×10^{-2} (kg/min)	Air flow rate 1.981×10^{-2} (kg/min)
200-250 µm	$u/u_{mf}=2.644\times10^{-5}\times T^{1.666}$	$u/u_{mf}=2.890\times10^{-5}\times T^{1.666}$	$u/u_{mf}=3.217\times10^{-5}\times T^{1.666}$
250-315 µm	$u/u_{mf}=1.810\times10^{-5}\times T^{1.666}$	$u/u_{mf}=1.976\times10^{-5}\times T^{1.666}$	$u/u_{mf}=2.200\times10^{-5}\times T^{1.666}$
315-400 µm	$u/u_{mf}=1.719\times10^{-5}\times T^{1.666}$	$u/u_{mf}=1.879\times10^{-5}\times T^{1.666}$	$u/u_{mf}=2.091\times10^{-5}\times T^{1.666}$
400-500 µm	$u/u_{mf}=1.636\times10^{-5}\times T^{1.666}$	$u/u_{mf}=1.789\times10^{-5}\times T^{1.666}$	$u/u_{mf}=1.991\times10^{-5}\times T^{1.666}$

It was noticed after analysing the dry mole fractions of CO_2, CO and O_2 that the combustion of propane usually accelerates for temperatures of reactant mixture above 500 or 600 ºC. Above this range, it is possible to detect four simultaneous phenomena: the generation velocities of CO_2 and CO accelerate sharply; the consumption of O_2 rises sharply; the noise level yielded by the combustion also increases sharply. These four phenomena occur owing to auto-ignition of reactant mixture in the fluidized bed.

In a closed vessel where there is a homogeneous mixture of air and propane at one atmosphere, the auto-ignition temperature is 480 ºC, Monnot (1978). However, in all 240 tests, the auto-ignition temperature was found to be higher. This happens because the free radicals in a fluidized bed are more likely to collide with a solid surface than inside a closed vessel. These wall collision reactions entail heterogeneous chain termination reactions, (De Soete, 1976; Turns, 2000), disrupting the kinetic mechanism of combustion inside the bed, Dennis et al. (1982).

The mole fractions of CO_2, CO and O_2 in the dried flue gases were measured and plotted towards the fluidized bed temperatures. The graphs were organized into four different types, according to the evolution of the CO_2, CO and O_2. Fig. (1) represents schematically these four types of graphs, with the corresponding CO_2, CO and O_2 evolutions. In some cases, the values shown in y-axis indicate the peak value that can be attained by the mole fraction considered. For curves type III and IV, there is a disturbance around 750 ºC, which will be explained later.

Table (3) presents the types of curves obtained for all performed tests. The types of graphs of Fig. (1) are mostly a function of the sand size and the depth of the fluidized bed. In the table there are cells with more than one type of graph assigned. In such cases the frequency of appearance of the type of graph diminishes from the left to the right, in the sequence contained in those cells.

Graphs of type I are typical of situations when propane burns with the smaller sand sizes and for $H_{mf} < 20$ cm, Tab. (3). The dry mole fraction of CO_2 increases with the temperature of fluidized bed after the auto-ignition; the dry mole fraction of CO drops to zero beyond 750-800 ºC; the dry mole fraction of O_2 decreases as the temperature increases, which is in line with the increase of production of CO_2 as the temperature of the fluidized bed increases, see Fig. (1).

Graphs of type II are associated with the higher sand sizes and 10 cm $< H_{mf} < 20$ cm. The dry mole fraction of CO_2, at the moment of auto-ignition, rises sharply from 0 to around 5-6 %, and remains constant thereafter. The dry mole fraction of CO attains a peak at the temperature of auto-ignition and becomes almost zero for higher temperatures. The dry mole fraction of O_2 is 20.8 % up to the auto-ignition, drops abruptly to 8-11 % and stays around this value after the auto-ignition. As the sand size increases, the gas-solid contact surface in the particulate phase drops and the probability of free radicals generated inside the bubbles of avoiding wall collision reactions, after being transferred to the particulate phase, increases too. Since the number of radicals in the particulate phase increases, the acceleration effect of these radicals is enhanced when they re-enter the bubbles.

Table 3. The ratio $u/u_{mf}(T)$ for all situations experimentally studied.

H_{mf} (cm)	Curve types			
30	III	III/IV	III/IV	III/IV
25	III	I/III	I/II/IV	I/III/II/IV
20	I	I/II	I/II	I/II/IV
15	I	I/II	I/II	II/I/III
10	I	I/II	I/II	II/I
Sand size (μm)	−250+200	−315+250	−400+315	−500+400

Curves Type I
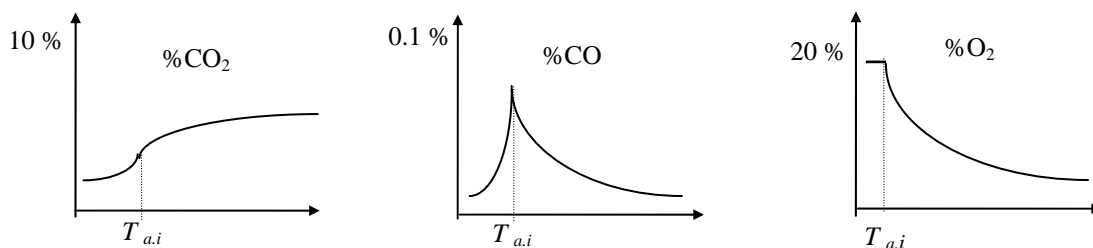
Curves Type II
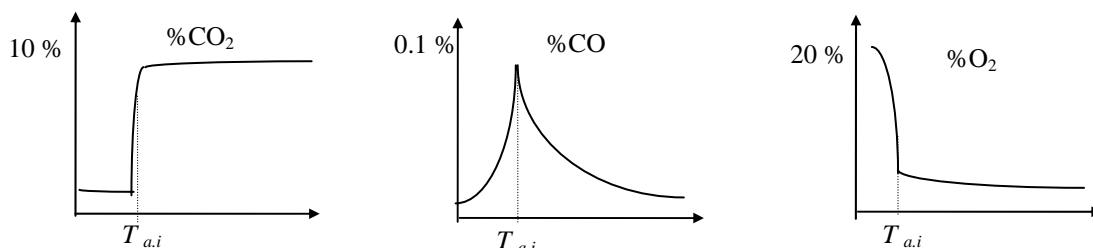
Curves Type III
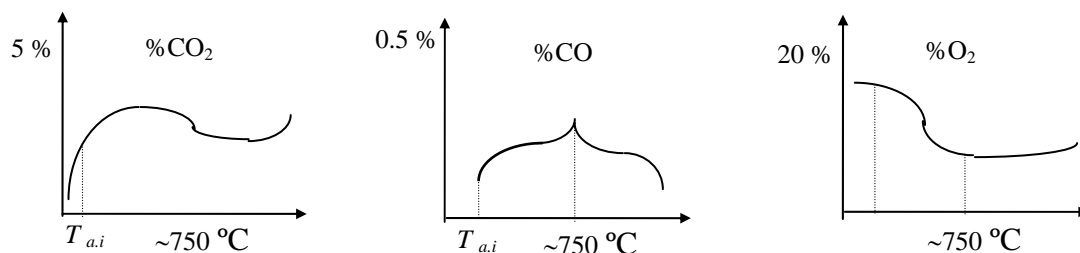
Curves Type IV
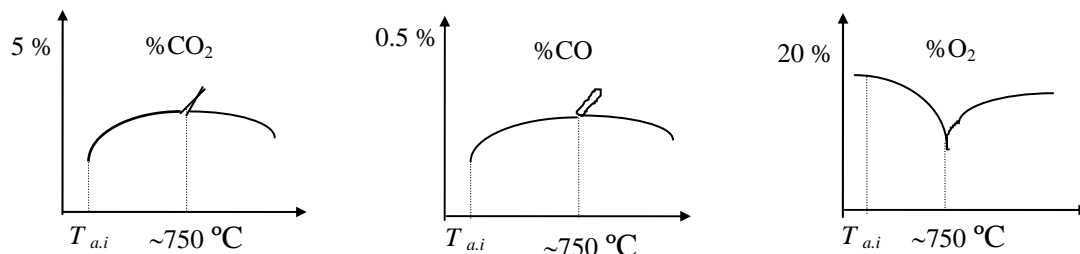
Figure 1. Curve types of dry mole fractions against the fluidized bed temperature.

Type III graphs are related with $H_{mf} > 20$ cm. The dry mole fraction of CO_2 rises slightly after the auto-ignition of the mixture, around 600-650 ºC, up to 5-7 % attained at about 700-750 ºC. The dry mole fraction of CO increases with temperature from the auto-ignition up to 700 ºC; at this temperature, the dry mole fraction of CO drops slightly, and resumes rising at 700 ºC up to 750 ºC, where it attains a peak; beyond 700-750 ºC the dry mole fraction of CO decreases slightly with temperature until it becomes almost zero, above 850 ºC.

As seen in graphs of either type I or type II, the peak of dry mole fraction of CO in the off gases coincides with the auto-ignition of the mixture. The most interesting feature of the graphs of type III consists in that the peak of dry mole fraction of CO in the off gases occurs about 100 ºC above the auto-ignition temperature. This is likely a consequence of the appearance of slugs inside the fluidized bed, which entails a mixing of packs of sand among bed regions at different temperatures. The result is a sharp drop of the temperature of the fluidized bed in the formerly hotter zones and the partial quenching of the combustion. This explains the peak of dry mole fraction of CO about 100 ºC beyond the auto-ignition temperature.

Type IV graphs only appear for beds with $H_{mf} \geq 25$ cm, Tab. (3). Typical curves of CO_2, CO and O_2 mole fraction against the temperature of the fluidized bed are shown in Fig. (2). In this graph there is a feature not found in the previous situations, the disturbance that appears in the curves around 750 ºC. For a deep bed, when the temperature reaches 750 ºC its value drops steeply to 730 ºC, and thereafter it resumes increasing. This disturbance is due to the appearance of slugs whose ascensions induce transfer of portions of sand between hotter and colder zones of the fluidized bed. In the shallow fluidized beds there are no slugs, so the curve of temperature against heating time has a shape without disturbances, Ribeiro and Pinho (2004).
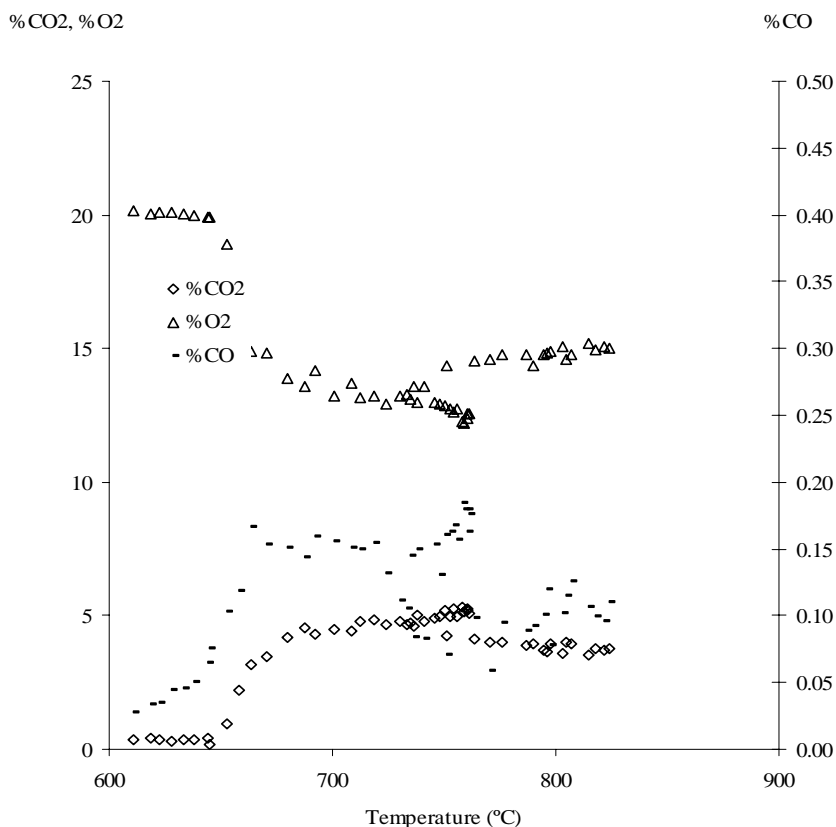
Figure 2. Mole percentage of CO_2, CO and O_2 against temperature of the fluidized bed. $H_{mf} = 30$ cm; sand size: 315-400 µm; air and propane with 30 % of excess air; air: 1.628×10^{-2} kg/min; propane: 8.299×10^{-4} kg/min. $u/u_{mf} = 1.719 \times 10^{-5} \times T^{1.666}$, with T in Kelvin.

It was noticed that, for a given temperature, a fluidized bed yields more CO as its depth increases. All CO in flue gases is generated inside the bubbles, and is partially transferred by diffusion and advection from the bubbles to the particulate phase. If inside the bubbles the hydrocarbons disappear, then the existing CO will be converted in CO_2, while the CO existing in the particulate phase must remain unchanged owing to the quenching of reactions. Therefore, for a given temperature and provided the bubbles only explode above the free surface of the fluidized bed, the bed yields more CO as its height increases, because bubbles have more time to generate CO and to transfer it to the particulate phase. If a bubble explodes inside the fluidized bed, its yielding of CO will increase as the time elapsed after its formation at the distributor up to its explosion, increases.

2.2. Combustion of pre-mixtures of propane and air in a silica sand fluidized bed with hematite

It was also studied the combustion of air propane mixtures in fluidized beds, but with the catalyst hematite. The composition of the flue gases and the sound level at the freeboard were measured and recorded. The results obtained with the reactor containing just sand were compared with homologous results obtained in the same reactor containing the mixture of hematite and sand. The bed material was silica sand of 400-500 μm and the hematite grain size was of 420-500 μm. The mass fraction of hematite in the particulate phase was 5%. Five static bed heights were considered: 10, 15, 20, 25 and 30 cm. The value of H_{mf} was considered equal to the static height of the fluidized bed. Only one flow rate of reactant mixture was used in all experiments, corresponding to a stoichiometric mixture: 1.073×10^{-6} kg/min of propane and 1.628×10^{-2} kg/min of air.

From the experiments no clear influence was found of the use of hematite upon the auto-ignition temperature of the gaseous reactant mixture, Table (4). However when there is hematite in the bed, combustion always started inside the bed whereas without hematite combustion always started above the bed free surface and only after the bed temperature reached the critical value, the reaction moved inside the particulate phase.

Table 4. Characteristic bed temperatures. Without (nh) and with (wh) hematite.

Bed depth [cm]	Auto-ignition temperature (nh) [ºC]	Critical temperature (nh) [ºC]	Auto-ignition temperature (wh) [ºC]
10	623 to 632	940	601 to 602
15	546 to 550	930	547 to 550
20	546 to 554	770	560
25	564	740	428
30	619	730	not measured
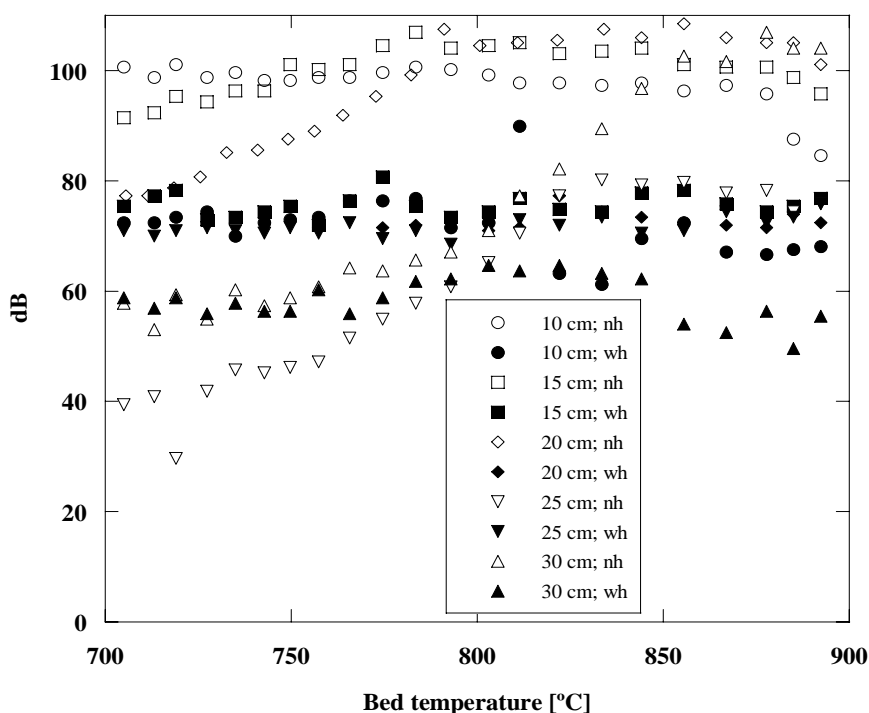
Figure 3. Noise level in function of the temperature of the fluidized bed for all tested bed depths, without (nh) and with (wh) hematite.

It was observed visually that without hematite and between the auto-ignition temperature and the critical temperature, violet flames stood above the bed, and disappeared when the bed critical temperature was reached. On the other hand, with hematite in the bed, no clear distinction between auto-ignition and critical temperature could be detected. In such circumstances the combustion always took place inside the bed, and the noise level was always around 70 dB.

As far as combustion noise and exhaust gases composition during normal combustion are concerned, in the present work only data obtained in the temperature range of 700 to 900 ºC, where the combustion is already well developed, are analysed and discussed. It was noticed that the sound level yielded by the combustion is louder for all experiments without hematite for beds of 10, 15 and 20 cm depth. For the 25 cm depth bed the sound level is almost equal for both situations whereas for the deeper bed, 30 cm, the combustion with hematite is noisier, Fig. (3). It can be said that when

there is hematite in the solid phase the combustion noise is around 70 dB for all bed temperatures in the 700 to 900 ºC range. During all the experiments with hematite the characteristic crackling of the combustion of gaseous mixtures in fluidized beds was not heard. At the free board it was not seen either explosions of bubbles or a continuous violet flame. In fact, the colour of the free surface was always bright orange.

The dry mole fractions of CO_2 and CO in the exhaust gases at the free board are higher when in the particulate phase there is hematite compared with the case when the particulate phase only contains sand, Figs. (4) and (5). The presence of hematite in the particulate phase tends to accelerate the chemical reactions of combustion. Indeed, the hematite tends to speed up the auto-ignition of the mixture; on the other hand, with hematite it is likely that bubbles will explode near the distributor on account of the low level of noise yielded by the combustion. Besides, as the particles of hematite stay outside the bubbles, then if the concentrations of CO_2 and CO in the off gases at the free board increase when in the particulate phase there is hematite, such increase is owing to the fact that the kinetic mechanism is not completely quenched in the particulate phase.
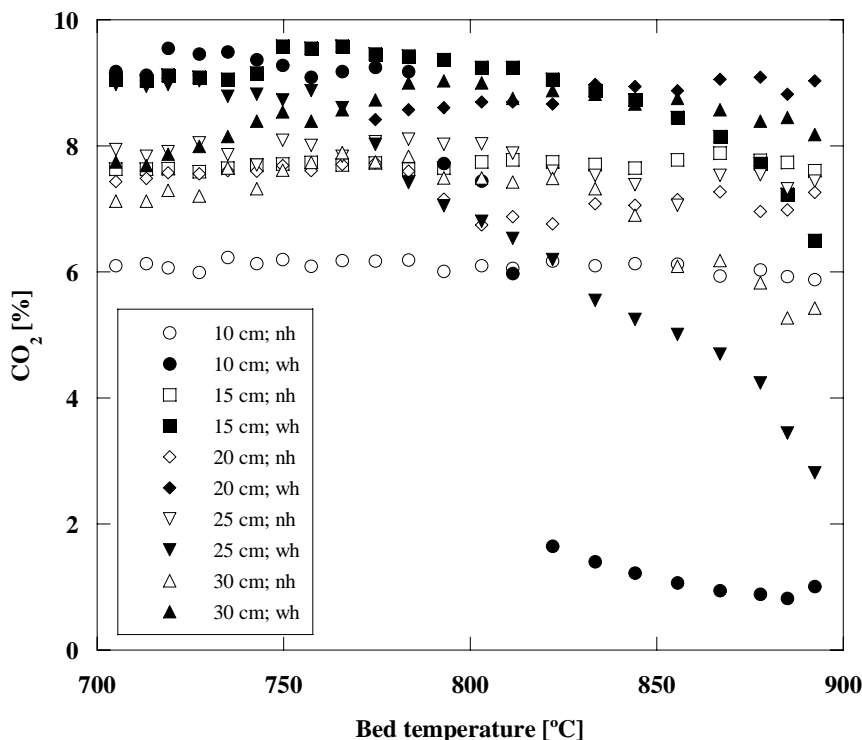
Figure 4. %CO_2 function of the fluidized bed temperature for all tested depths, without (nh) and with (wh) hematite.

3. Mathematical model

A mathematical model is proposed to show the evolution of temperature, chemical composition and energy release or transfer in bubbles, clouds and particulate phase, in a fluidized bed where there are bubbles, of a mixture of air and propane, moving up through the particulate phase. The analysis begins as the bubbles are formed at the orifices of the distributor, until they explode inside the bed or emerge at the free surface. The model also analyses of what happens in the gaseous mixture that leaves the free surface of the fluidized bed until the propane is thoroughly burnt. It is essentially built upon a simple quasi-global mechanism for the combustion reaction and the mass and heat transfer equations from the two-phase model of fluidization. The aim was not to propose a new modelling approach, but to combine classical models, one concerning the reaction kinetics and the other the bed hydrodynamic aspects, to obtain a better insight on the events occurring inside a fluidized bed reactor. Experimental data to validate the numerical model were obtained through tests on the combustion of commercial propane, in a laboratory scale fluidized bed, using four sand particle sizes: 400-500, 315-400, 250-315 and 200-250 µm. The mole fractions of CO_2, CO and O_2 in the flue gases and the temperature of the fluidized bed were measured and compared with the numerical results.

The philosophy adopted consisted in the coupling of classic and well established models for the overall kinetics of combustion and for the hydrodynamics of the bed. The global kinetic mechanism for the combustion of hydrocarbons proposed by Hautman *et al.* (1981) was chosen; besides, as the backbone for the bed hydrodynamics, it was chosen the classic two phase theory of fluidization of Davidson and Harrison (1963), although it was followed the approach of Kunii and Levenspiel (1990). Although more recent global kinetic mechanisms for the combustion of hydrocarbons could be applied, they all follow the same basic assumptions, as can be seen in the review of Westbrook and Dryer (1981), and the final result is not at all different from what can be obtained through the adopted mechanism.
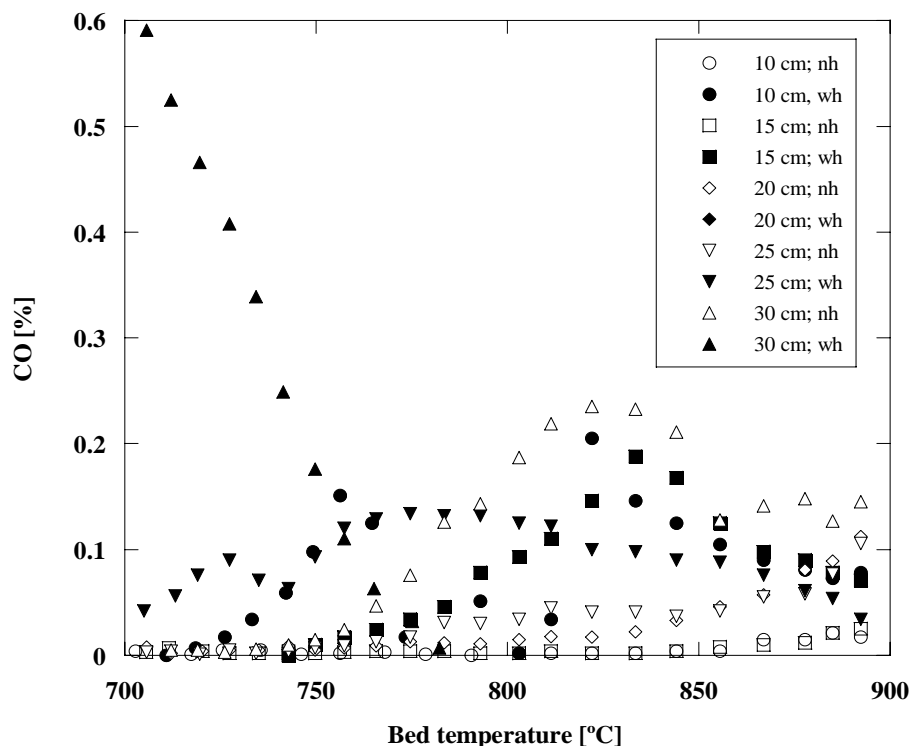
Figure 5. %CO function of the fluidized bed temperature for all tested depths, without (nh) and with (wh) hematite.

The kinetic mechanisms do not proceed in the particulate phase owing to quenching by heterogeneous reactions, Aoyagi and Kunii (1974), Ribeiro and Pinho (2004). So, it will be assumed that the kinetic mechanisms only proceed within the bubbles, and are quenched outside them. Besides, the rising of the bubbles along the fluidized bed entail intense advection of sand in the particulate phase, and therefore the particulate phase will be considered as well stirred.

As a result of the turbulence created inside the bubbles by cross flow, it will be assumed in this model that the gaseous mixture inside the bubbles is well stirred. The chemical composition of the bubbles will then be a function of the time elapsed since they were generated at the distributor.

The adopted global kinetic mechanism for the combustion of mixtures of air and propane is composed by the following four reactions, Hautman et al. (1981),

$$C_3H_8 \rightarrow 1.5C_2H_4 + H_2, \tag{1}$$
$$C_2H_4 + O_2 \rightarrow 2CO + 2H_2, \tag{2}$$
$$CO + 0.5O_2 \rightarrow CO_2, \tag{3}$$
$$H_2 + 0.5O_2 \rightarrow H_2O. \tag{4}$$
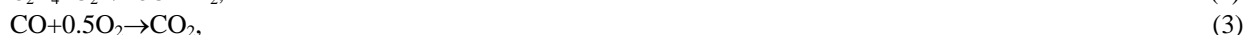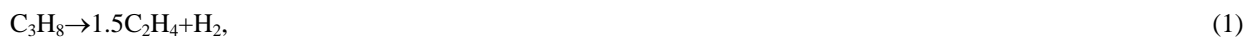
The authors also proposed equations to evaluate the rate of each of the previous four chemical reactions. These rate equations were integrated using a fourth order Runge-Kutta numerical scheme.

Bubbles in a fluidized bed are surrounded by clouds and outside these clouds there is the particulate phase. The chemical species generated inside a bubble are transferred to the cloud by two processes: diffusion and advection of gas between the cloud and the bubble. The overall mass transfer coefficient of species i between a bubble and the respective cloud, $(K_{bn})_b(i)$, based on the volume of the bubble, is given by, Kunii and Levenspiel (1990),

$$\left(K_{bn}\right)_b (i) = 4.5 \frac{u_{mf}}{D_e} + 5.85 \frac{D_{Ei-N2}^{0.5} g^{0.25}}{D_e^{1.25}} \tag{5}$$

where u_{mf} is the incipient fluidization velocity, D_e is the equivalent diameter of the bubble and D_{Ei-N2} is the diffusivity of species i on N_2. The equivalent diameter D_e of the bubbles existing in the fluidized bed at the level z, measured from the distributor, can be evaluated through, Darton et al. (1977),

$$D_e = 0.54 \left(u - u_{mf}\right)^{2/5} \left(z + 4.0\sqrt{A_0}\right)^{4/5} g^{-1/5}. \tag{6}$$

where A_0 is the distributor area per each orifice and u is the superficial velocity of the gas crossing the reactor.

The bubbles contain many chemical species that are represented by a set of eight species, C_3H_8, C_2H_4, CO_2, CO, H_2, O_2, H_2O and N_2, Hautman et al. (1981). It was assumed that the diffusivity of species E_i from a bubble to its cloud is nearly the diffusivity of species E_i to N_2, D_{Ei-N2}, Kanury (1977) and Borman and Ragland (1998). Therefore, the concentrations of chemical species existing inside bubbles at the instant t, evaluated through the rate equations of the kinetic mechanism, must be corrected in order to account for the mass transfer between bubbles and their clouds during the time interval Δt. It means that two physically simultaneous phenomena were mathematically uncoupled: one of these phenomena consists on the generation of species owing to the kinetic mechanism; the other consists on the species transfer from bubbles to their surrounding clouds. That separation will be more accurate as Δt diminishes.

There is also mass transfer between the clouds and the particulate phase. The mass transfer occurs only by diffusion, and the overall mass transfer coefficient between a cloud and the particulate phase for species i, based on the volume of the bubble, $(K_{ne})_b(i)$, is given by, Kunii and Levenspiel (1990),

$$\left(K_{ne} \right)_b \left(i \right) \approx 6.78 \left(\frac{\varepsilon_{mf} D_{Ei-N_2} u_b}{D_e^3} \right)^{0.5} \tag{7}$$

The rate of temporal variation of the concentrations of chemical species in the particulate phase was obtained through a balance for a generic species E_i: the temporal variation of the number of moles of E_i in the particulate phase equals the difference between the mole flow-rate of E_i that enters the particulate phase through the distributor, and the mole flow-rate of E_i that leaves the particulate phase through the free surface of the fluidized bed, plus the mole flow-rate of E_i that issues from the clouds into the particulate phase.

The temperature of a bubble changes because: (i) among the set of reactions, Eqs. (1) to (4), the first is endothermic while the other three are exothermic; (ii) there is heat transfer by conduction between bubbles and clouds and particulate phase; (iii) there is mass transfer between bubbles and clouds. The overall heat transfer coefficient between a bubble and its surrounding cloud, based on the volume of the bubble, is given by, Kunii and Levenspiel (1990),

$$\left(U_{bn} \right)_b = 4.5 \left(\frac{u_{mf} \rho_b c_{pb}}{D_e} \right) + 5.85 \frac{\left(\lambda_b \rho_b c_{pb} \right)^{1/2} g^{1/4}}{D_e^{5/4}} \tag{8}$$

The thermal conductivity of the gas of a bubble λ_b, was considered equal to the thermal conductivity of the air. This was done because the gas of the bubbles is not very much different from air.

The temperature of the bubbles was evaluated by

$$\rho_b c_{pb} \frac{dT_b}{dt} = Q \tag{9}$$

where $\rho_b c_{pb}$ is the calorific capacity of the bubble and Q encompasses the net calorific power per volume of bubble generated by all chemical reactions occurring inside the bubble and the net calorific power entering into the bubble owing to heat conduction and cross-flow. The mathematical model evaluated the temperature of the bubble at the instant $t+\Delta t$ with the temperature of the bubble at t and the value of Q corresponding to the net calorific power of the bubble during Δt.

As stated before the bubbles can explode inside the fluidized bed. From the model of Hautman *et al.* (1981) it can be concluded that these explosions are triggered by the disappearance of propane in the bubbles, which in turn entails the disappearance of intermediate hydrocarbons in the bubbles at, theoretically, infinite velocity. If inside the bubbles there is enough amount of oxygen, the intermediate hydrocarbons will be converted suddenly and thoroughly into carbon monoxide and hydrogen, Eq. (2). If inside the bubbles there is not enough oxygen for the complete oxidation of intermediate hydrocarbons according the reaction (2), the proposed model will assume that intermediate hydrocarbons will be converted into carbon monoxide and hydrogen until the extinction of oxygen, which means that in this case there will be intermediate hydrocarbons unburned inside the bubbles after the explosions. The model of Hautman *et al.* (1981) predicts that the extinction of intermediate hydrocarbons triggers the extinction of hydrogen at very high velocity. If inside the bubbles after the complete oxidation of intermediate hydrocarbons there is enough amount of oxygen to burn hydrogen, then the hydrogen will be converted suddenly and totally into water, Eq. (4). If inside the bubbles there is not enough oxygen for the complete oxidation of hydrogen according to Eq. (4), then the model will assume that hydrogen will be converted into water until the extinction of oxygen, which entails that in this case there will be unburned hydrogen inside the bubbles after the explosions.

When bubbles explode inside the fluidized bed, the matter that constitutes them will be thrown away in all directions and at high speed. Hayhurst (1991) noticed that from that matter thrown away results new bubbles. Since the chemical composition of these new bubbles is equal to the chemical composition of the original ones, then the equivalence ratio of the mixture of the new bubbles should be very high. So, the velocity of combustion of CO will be

very slow inside the new bubbles and it is plausible to assume that the kinetic mechanism is frozen inside these new bubbles. In the particulate phase, it was already said that this mechanism is frozen. Therefore, the proposed model neglects everything that eventually happens since the bubbles explode inside the fluidized bed until they surface. When the bubbles surface, the model assumes that the gas from bubbles mixes adiabatically and at constant pressure with the gas leaving the fluidized bed from the particulate phase

The number of moles of chemical species existing in bubbles when these bubbles surface, was obtained multiplying the species concentration [$E_i b(t_{expl.})$], by the total volume of bubbles with age t, $V_{b-total}$, evaluated according Mori and Wen (1975), by

$$V_{b-total} = 2.300 \left[A \left(u - u_{mf} \right) \right]^{6/5} \tag{10}$$

If the bubbles do not explode inside the fluidized bed the model assumes that gases from bubbles mix adiabatically and at constant pressure with gases coming from the particulate phase at the free surface of the fluidized bed. The rising time of bubbles across the fluidized bed t_{sub}, was evaluated by the following equation, Ribeiro and Pinho (1998),

$$t_{sub} = \frac{H}{\overline{U}_b} = \frac{H^2}{\left(u - u_{mf} \right) H + 0.93 \left(u - u_{mf} \right)^{1/5} \left[\left(H + 4\sqrt{A_0} \right)^{7/5} - \left(4\sqrt{A_0} \right)^{7/5} \right]} . \tag{11}$$

Above the free surface of the fluidized bed the model applies the kinetic mechanism of Hautman et al. (1981) to the mixture of gas from bubbles and of gas from the particulate phase.

The initial concentrations of propane, oxygen and nitrogen in the bubbles were calculated with the flow-rates of propane and air, assuming that the bubbles were at atmospheric pressure and initially at the environment temperature. For the intermediate hydrocarbons, C_2H_4 in the model, and for CO, H_2 and H_2O, initial concentrations different of zero were considered. It was adopted as the initial concentrations for all these species one thousandth of the initial concentration of propane. The rising of the bubbles along the fluidized bed entails intense advection of sand in the particulate phase, and therefore the particulate phase will be considered as well stirred. For this phase, the initial concentrations for C_3H_8, C_2H_4, CO_2, CO, H_2 and H_2O were taken as zero; the initial concentrations for N_2 and O_2 were the same as in the environment.

The computer program can perform calculations until the complete combustion of fuel, but it was assumed that the chemical reactions are quenched at the instant when the calculated dry mole fractions of CO_2, CO and O_2, on the flue gases leaving the fluidized bed, are the closest to the homologous measured values.

4. Numerical results

For each of the four sand particle sizes used in this study were done twelve simulations covering three different bed temperatures (973, 1073 and 1173 K), four bed heights (0.1, 0.15, 0.2 and 0.25 m), for the same reactant volumetric flow rate (2.3518×10⁻⁴ m³/s), under stoichiometric conditions. The discussion herein concerns only the temperatures inside the bubbles obtained for just three of those simulations, for the sand size of 400-500 μm. Data corresponding to these three simulations are given in Tab. (5). These three cases are paradigmatic of the situations that can occur during the combustion of a gaseous mixture of air and propane in a fluidized bed: explosion of bubbles above the free surface of the fluidized bed, near the free surface of the fluidizing bed, and inside the fluidized bed.

Table 5. Conditions for the numerical simulations.

		Simulation 1	**Simulation 2**	**Simulation 3**
u_{mf} (20 ºC, 101325 Pa)	m/s	3.01×10^{-4}	3.01×10^{-4}	2.20×10^{-4}
u/u_{mf}	-	1.56	1.56	2.12
H_{mf}	m	0.10	0.25	0.10
T	K	973	973	1173
V_{mist} (20 ºC, 101325 Pa)	m³/s	2.3518×10^{-4}	2.3518×10^{-4}	2.3518×10^{-4}

Figure (6) shows the evolution of temperature of the bubbles, as they rise inside the bed, for the three simulations under analysis. In simulation 1 the temperature of the bubbles diminishes as the bubbles rise along the fluidized bed. This temperature drop can be understood with the balance of the energy generated per volume of bubble through the exothermic chemical reactions (2), (3) and (4) and the endothermic reaction (1), as well as the energy per volume of bubble transferred by the bubbles to clouds and to the particulate phase. The sum of all these energetic components is negative. It can be seen through the curve for simulation 2 that the temperature inside the bubbles drops as these bubbles rise until about 0.15 m; above this level the temperature of bubbles increases slightly. The initial drop of the temperature of bubbles occurs because the cooling effect of endothermic reaction (1) outweighs the heating effect of

reactions (2), (3) and (4), which are exothermic. Above the level 0.15 m the exothermic reactions accelerate the release of heat. For simulation 3 the bubbles of reactant mixture explode approximately at the level 0.0025 m, inside the fluidized bed, near the distributor. When bubbles explode, the energy absorbed by reaction (1) increases swiftly up to a peak, and after this peak it drops to zero almost instantaneously. That increase of energy release occurs because the propane existing inside the bubbles breaks at high speed during explosion and generates intermediate hydrocarbons; the ensuing drop of energy release is owing to the disappearance of propane during explosion of bubbles. The explosion is induced by the large production of thermal energy through reactions (2), (3) and (4).
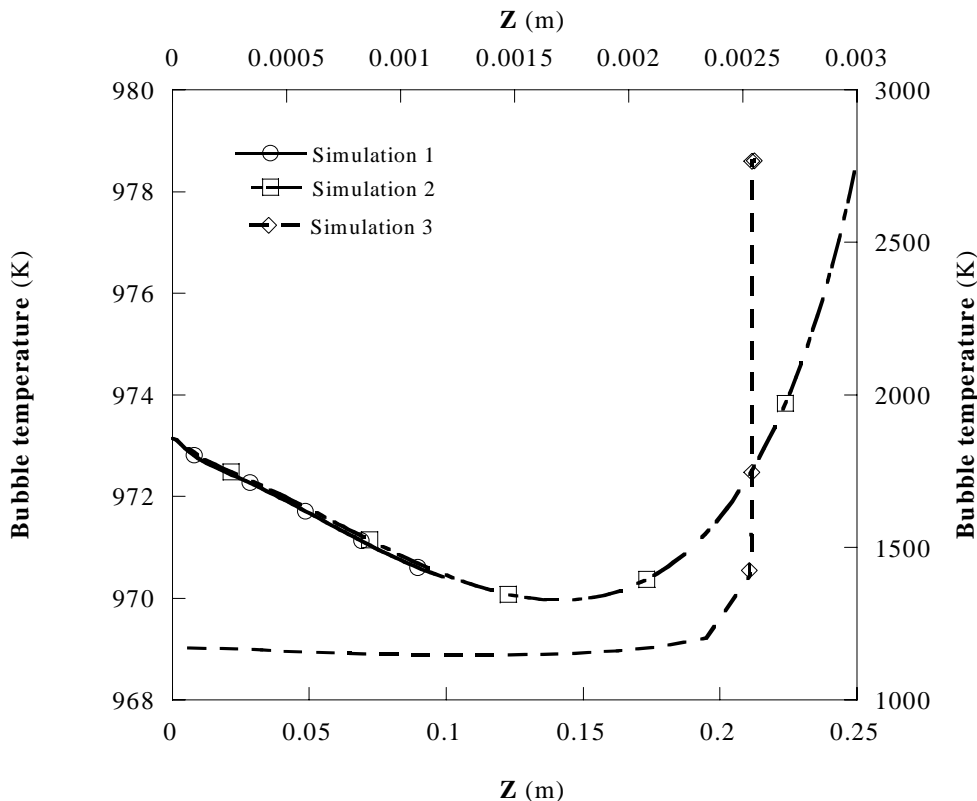
Figure 6. Temperature of the bubbles. Simulations 1 and 2 refer to the lower abscissa and the left ordinate axis. Simulation 3 refers to the upper abscissa and the right ordinate.

Table 6. Comparison among measured and calculated values for dry mole fractions of gaseous species.

	Calculated values				Measured values		
Simulation	Temperature	CO_2	CO	O_2	CO_2	CO	O_2
-	K	%	%	%	%	%	%
1	2199	6.39	0.01	10.34	5.9	0.008	12.0
2	2210	6.55	0.04	10.08	7.0	0.04	10.0
3	2226	6.06	0.003	10.84	6.5	0.003	11.5

4.4 Comparison between measured and calculated values

In Tab. (6) are presented the calculated and the measured values for the situations of simulations 1, 2 and 3. The computer program can perform calculations until the complete combustion of fuel, but it was assumed that the chemical reactions are quenched at the instant when the calculated dry mole fractions of CO_2, CO and O_2, on the flue gases leaving the fluidized bed, are the closest of the homologous measured values.

The departure between calculated and measured dry mole fractions of CO_2, CO and O_2 in the flue gas seldom exceeds 10 % of the measured value, for all studied situations.

4.4 Conclusions

Results of experimental and numerical experiments concerning the overall behaviour of commercial propane combustion in a laboratory scale bubbling fluidized bed reactor were presented. The importance of using a low cost catalyst on pollutants emission and noise reduction was shown.

The simple numerical model allowed a better understanding of the combustion reactions taking place inside the bubble phase. A close approach was obtained among measured and calculated gas dry mole fractions at bed exit.

6. References

Aoyagi, M. and Kunii, D., 1974, "Importance of dispersed solids in bubbles for exothermic reactions in fluidized beds", Chem. Eng. Commun., pp. 191-197.

Borman, G.L. and Ragland, K.W., 1998, "Combustion Engineering", McGraw-Hill International Editions.

Bulewicz, Elzbieta M., Kadenfer S. and Pilawska M. (1997), "Natural gas combustion in a bed of sand", Fluidized Bed Combustion, Vol. 2, ASME 1997.

Darton, R. C., LaNauze, R.D., Davidson, J.F. and Harrison , D., 1977, "Bubble Growth Due to Coalescence in Fluidized Beds", Trans. I. Chem. E., Vol. 55, p. 274-279.

Davidson, J. F., and Harrison, D., 1963, "Fluidised particles", Cambridge University Press of Cambridge.

De Soete, G., 1970, "Aspects fondamenteaux de la Combustion en phase gazeuse", Editions Technip, Paris.

Dennis, J. S., Hayhurst A.N. and Mackley, I.G., 1982, "The Ignition and Combustion of Propane/Air Mixtures in a Fluidized Bed", Nineteenth Symposium (International) on Combustion, The Combustion Institute, p. 1205-1212.

Geldart, D., 1986, "Gas Fluidization Technology", John Wiley and Sons Ltd.

Gokulakrishnan, P., Lawrence, A. D., 1999, "An experimental study of the inhibiting effect of chlorine in a fluidized bed combustor", Combustion and Flame, Vol. 116, p. 640-652.

Hautman, D. J., Dryer, F. L., Schug, K. P. and Glassman, I., 1981, "A multiple-step overall kinetic mechanism for the oxidation of hydrocarbons", Combustion Science and Technology, Vol. 25, p. 219-235.

Hayhurst, A. N., 1991, "Does Carbon Monoxide Burn Inside a Fluidized Bed? A New Model for the Combustion of Coal Char Particles in Fluidized Beds", Combustion and Flame, Vol. 85, p. 155-168.

Hayhurst, A. N., Lawrence, A. D., 1996, "The effect of solid CaO on the production of NO_x and N_2O in fluidized bed combustors: studies using pyridine as a prototypical nitrogenous fuel", Combustion and Flame, Vol. 105, p. 511-527.

Hayhurst, A N. and Lawrence, A. D., 1997, "The reduction of nitrogen oxides NO and N_2O to molecular nitrogen in the presence of iron, its oxides, and carbon monoxide in a hot fluidized bed". Combustion and Flame, Vol. 110, p. 351-365.

Hayhurst, A N. and Parmar, M. S., 1998, "Does solid carbon burn in oxygen to give the gaseous intermediate CO or produce CO_2 directly? Some experiments in a hot bed of sand fluidized by air", Chemical Engineering Science, Vol. 53, N 3, pp. 427-438.

Hayhurst, A N. and Tucker, R. F., 1990, "The combustion of carbon monoxide in a two-zone fluidized bed", Combustion and Flame, Vol. 79, pp. 175-189.

Hesketh, R. P. and Davidson, J. F., 1991a, "The effect of volatiles on the combustion of char in a fluidised bed", Chemical Engineering Science, Vol. 46, N 12, pp. 3101-3113.

Hesketh, R. P. and Davidson, J. F., 1991b, "Combustion of methane and propane in an incipiently fluidized bed", Combustion and Flame, Vol. 85, pp. 449-467.

Kanury, A. M., 1977, "Introduction to Combustion Phenomena", Gordon and Breach Science Publishers.

Kunii, D. and Levenspiel, O., 1990, "Fluidization Engineering", Butterworth-Heinemann.

Monnot, G., 1978, "La Combustion dans les fours et les chaudières", Editions Technip.

Mori, S., and Wen, C. Y., 1975, "Estimation of bubble diameter in gaseous fluidized beds", A.I.Ch.E. Journal, Vol 21, N 1, p. 109-115.

Pillai, K. K., 1981, "The influence of coal type on devolatilization and combustion in fluidized beds", Journal of the Institute of Energy, Vol. 142, pp. 142-150.

Ribeiro, L. and Pinho, C. M. C. T., 1998, "Combustion of propane and methane in the bubbles of a fluidized bed", Symposium on Thermal and Fluids Engineering, CSME Forum´98, Vol. 1, pp.33-40, Toronto, Ontario, Canada.

Ribeiro, L. and Pinho, C., 2004, "Generic Behaviour of Propane Combustion in Fluidized Bed", Chemical Engineering Research and Design, Vol. 82 (A12), p. 1597-1603.

Stubington, J. F., Chan, S. W. and Clough, S. J., 1990, "A model for volatiles release into a bubbling fluidised bed combustor", A.I.Ch.E. Journal, Vol. 36, pp. 75-85.

Turns, S. R., 2000, "An Introduction to Combustion", McGraw-Hill International Editions.

Westbrook, C. K., Dryer, F. L., 1981, "Simplified reaction mechanisms for the oxidation of hydrocarbon fuels in flames", Combustion Science and Technology, Vol. 27, p. 31-43.

Williams, F.A., 1985, "Combustion Theory", 2nd edition, Perseus Books Publishing, Cambridge, Massachussets.